Analytical and Bioanalytical Chemistry (2018) 410:4645–4655
https://doi.org/10.1007/s00216-018-0878-0

RESEARCH PAPER

Dicationic ionic liquid thermal decomposition pathways

Rahul A. Patil[1] · Mohsen Talebi[1] · Alain Berthod[1,2] · Daniel W. Armstrong[1]

Received: 10 November 2017 / Revised: 4 January 2018 / Accepted: 12 January 2018 / Published online: 30 January 2018

Abstract
The rapid expansion in the study and use of ionic liquids (ILs) is a result of their unique properties including negligible volatility, high thermal stability, and ability to dissolve disparate compounds. However, because ILs have infinitely variable structures (often referred to as "tunability"), these properties can differ considerably. Herein, we focus on the thermal stability of 15 bis-/dicationic ionic liquids. Specifically, their thermal breakdown products are examined to determine the structural linkages, bonds, or atoms most susceptible to thermally induced changes and whether such changes occur before possible volatilization. In most cases, the heteroatom-carbon single bonds were susceptible to thermolytic decomposition.

Keywords Ionic liquid · High temperature · Decomposition mechanism · Thermal decomposition · Thermal stability

Introduction

Salts with melting points lower than 100 °C are referred to as ionic liquids (ILs) [1]. Since their rediscovery at the end of the last century, these innovative fluids found applications in different branches of chemistry such as liquid-liquid extraction [2], microextractions [3, 4], solvents for extraction of DNA [5, 6], mass spectrometry [7–10], electrochemistry [11, 12], spectroscopy [4, 13], high-performance liquid chr``omatography [14, 15], and capillary electrophoresis [16, 17]. Thanks to their extremely low vapor pressure, non-flammability, wide liquid temperature range, and high thermal stability, ILs have been successfully applied in high temperature environments (such as liquid thermal storage media [18], high-temperature lubricants [19, 20], lubricant additives [21, 22], solvents for high-temperature reactions [23–25], gas chromatography (GC) stationary phases [26–28], solvents for headspace GC [29–32], high-temperature non-flammable electrolytes for batteries [33]) and high vacuum environments (high-performance lubricating greases for space [34] and high vacuum lubricants [35, 36]). In fact, the IL thermal stability can vary considerably depending on the nature of the IL anion and cation. Bis- or dicationic, imidazolium-based or phosphonium-based ILs often show decomposition temperatures higher than traditional monocationic ILs [37, 38]. The anion also can play a significant role in the IL thermal stability, e.g., nucleophilic halogens can attack the cation moiety [37, 39].

The most striking features of ILs are their low volatilities and high thermal stabilities, compared to common organic solvents. There are several methods reported for determining thermal stabilities of ILs. The short-term IL thermal stability is determined by thermogravimetric analysis (TGA) using temperature ramps of 5–10 °C/min and measuring the temperatures of 5% weight loss (T_d) [38–40]. The T_d temperatures are useful to compare the thermal stabilities of different ILs [38]. Since thermal stability is a time-dependent process, different results may be obtained when ILs are exposed to thermal stress for longer periods [41]. The long-term thermal stability, determined by monitoring weight loss by isothermal TGA experiments, provides detailed information on the stabilities/volatilities and/or rates of decomposition of ILs [39]. In kinetic studies, determination of frequency factor and activation

---

Published in the topical collection *Ionic Liquids as Tunable Materials in (Bio)Analytical Chemistry* with guest editors Jared L. Anderson and Kevin D. Clark.

Electronic supplementary material The online version of this article (https://doi.org/10.1007/s00216-018-0878-0) contains supplementary material, which is available to authorized users.

✉ Daniel W. Armstrong
sec4dwa@uta.edu

[1] Department of Chemistry and Biochemistry, University of Texas at Arlington, 700 Planetarium Place, Arlington, TX 76019, USA

[2] Institut des Sciences Analytiques, Université de Lyon 1, CNRS, 5 rue de la Doua, 69100 Villeurbanne, France

energies, using the Arrhenius equation, provides information about the frequency of molecular collisions (collisions between cations and anions) and the proportion of collisions resulting in decomposition reactions respectively [42]. The long-term thermal stability is also determined by inverse gas chromatography, in which the column bleed is monitored by highly sensitive detectors as a function of temperature [27, 37, 38]. The observed mass loss upon heating can be due to volatilization (formation of neutral ion pairs (NIPs)) or to real thermal decomposition (TD) [39, 43]. Along with mass loss, ILs also can show color changes after heating at high temperatures, long storage times, and wear/friction in tribological applications which can be related to decomposition and formation of side products [23, 42, 44].

Most IL literature focuses on the determination of thermal stabilities, methods to determine thermal stabilities, rates of decomposition, etc. Little attention has been paid to the analysis of decomposition products, the reasons for weight loss, and color changes in ILs at higher temperatures. Recent reports have shown that the thermal stabilities of ILs can be altered by structural modifications [28, 38, 40, 45]. These reports compile trends of the "structure-thermal stability" relationships of ILs but do not provide any detailed explanation about the effects of various structural moieties on the IL decomposition. There are only a few reports on the thermal degradation products of some imidazolium and pyrrolidinium monocationic ILs [42, 46–48] and no reports on the analysis of decomposition products of dicationic ILs. The degradation studies of imidazolium-based monocationic ILs were done by pyrolysis GC-MS and established that the decomposition started by the removal of alkyl substituents on the imidazole ring [46, 47], while the monocationic pyrrolidinium-based ILs with cyano anions were observed to polymerize at higher temperatures [48].

Considering the popularity of dicationic ILs in high temperature applications, the results of a degradation study can be helpful for their optimal use, determining their changes at high temperatures and for providing information on possible structural modifications to further improve stability. The present work summarizes the results of a systematic and comprehensive thermal decomposition study performed on 15 bis(trifluoromethylsulfonyl)imide (NTf_2) dicationic imidazolium, pyrrolidinium, and phosphonium-based ILs at 400–440 °C. The effect of different linkages such as straight alkane chains, polyethylene glycol chains, and branched alkane chains on the thermal behavior of ILs also was evaluated via these degradation studies. The soft ionization technique, electrospray ionization mass spectrometer (ESI-MS), was used to avoid the further fragmentation of decomposition fragments and to identify them, in contrast to what can be accomplished with pyrolysis GC-MS.

Materials and methods

Instruments

The analyses were performed on a mass spectrometer Finnigan LXQ ESI-MS (Thermo Fisher Scientific, San Jose, CA). The ESI analysis conditions were as follows: spray voltage 4.5 kV, sheath gas flow rate 35, aux gas flow rate 6, capillary temperature 275 °C, capillary voltage 16 V, tube lens 110 V, scan range 50–1000 *m*/*z*, positive mode.

Materials

1-Benzyl-2-methylimidazole (90%), 1,2-dimethylimidazole (98%), *N*-methylpyrrolidine (97%), tripropylphosphine (97%), 1-(2-hydroxyethyl)imidazole (97%), 1,9-dibromononane (97%), 1,5-dibromopentane (97%), 3-bromo-2-bromomethyl-1-propene (97%), 1-bromo-3-(2-bromoethyl)-4,4-diethylpentane, 1,3-dibromobutane (97%), tetraethylene glycol (99%), phosphorus tribromide (99%), and bis(trifluoromethanesulfonyl)imide lithium salt (99.95%) were purchased from MilliporeSigma (ex-Sigma-Aldrich, St. Louis, MO). 1,5-Dibromo-3-methylpentane (98+%) was purchased from Alfa Aesar (Haverhill, MA). 1,5-dibromo-3,3-dimethylpentane (95%) was obtained from Alfa Chemistry (Holtsville, NY). 1,3-Dibromo-2-methylpropane (95+%) was purchased from Oakwood Chemicals (Estill, SC). The detailed procedures for synthesis of ILs are reported in the literature [38, 49, 50].

Experimental design

A weighed amount of each IL was introduced in a closed vessel that could be heated up to 400 °C. Argon was circulated through the vessel to carry any volatiles generated by the IL upon heating. These volatiles were trapped in a flask cooled to − 78 °C by an acetone-dry ice bath. After 30 min at 400 °C, the vessel was cooled, and the collection flask was disconnected. The heated IL was visually inspected, and 10-mL methanol was introduced into the container. The methanolic solution was collected and filtered for MS analysis for identification of non-volatile (residual) degradation products in the heated IL. Similarly, 10-mL methanol was added to the volatile-collection flask for analysis by direct infusion MS and identification of volatile degradation products (see Electronic Supplementary Material (ESM) section 1.1 for full details).

Results and discussion

Fifteen different dicationic ILs (IL1 to IL15), either di-imidazolium, di-pyrrolidinium, or di-phosphonium paired with bis(trifluoromethylsulfonyl)imide (NTf_2) anions were synthesized. Five dicationic ILs were made with a nonane (C_9) alkyl spacer, three with a polyethylene glycol (PEG, three units) spacer, three with branched C_3 spacers, one with a C_5 linkage spacer, and three with branched C_5 spacers [38, 49]. Their thermal behavior was tested as per the procedure outlined in the "Experimental design" section.

Analysis of straight chain linkage ILs

Table 1 lists the structure of the eight ILs, coded IL1 to IL8, along with, the three major peaks seen in the mass spectra of the residual ILs after 30 min heating at 400 °C, in decreasing intensity order. The mass spectra of the collected volatiles were much richer in peaks than those of the residual heated ILs. Table 2 lists similarly the four major peaks seen in the spectra of the collected volatiles along with the bonds broken to form these fragments. Figure 1 compared the mass spectrum of the original IL1 (Fig. 1a) with that of the 400 °C heated IL1 residue (Fig. 1b), and the corresponding spectrum of the collected IL1 volatiles after 30 min of heating at 400 °C (Fig. 1c).

On visual inspection, apart from some darkening, IL1 is practically unchanged after heating at 400 °C for 30 min. The mass spectrum of the heated IL1 is practically identical to the initial spectrum showing a very small 152 *m/z* peak, likely the result of *N*-methyl elimination (Fig. 1a, b). A color change is observed (see ESM Fig. S3), and trace amounts of volatiles were collected giving the Fig. 1c mass spectrum. As listed in Table 2, the 207 *m/z* peak corresponds to the loss of a dimethylimidazole group plus a methylene group. The possible mechanism for the loss of alkyl substituents on the imidazole ring is shown in Fig. 3. The loss of alkyl substituents on the imidazole ring due to the nucleophilicity of an anion, known as the "reverse Menshutkin reaction" was observed

Table 1 MS peaks of residual (non-volatile) dicationic NTf_2 ionic liquids seen after heating at 400 °C for 30 min under argon flow

IL code	Dication structure	Dication m.w.	T_d[a] °C	Peak 1		Peak 2		Peak 3	
				Mass	Broken bond	Mass	Broken bond	Mass	Broken bond
IL1	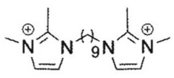	318.54	467[b]	Intact 318 (m/z 159)	None	Dication + NTf_2 598	None	Loss of methyl 304 (m/z 152)	C-N
IL2	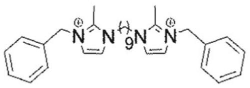	470.34	437[b]	Loss N benzyl 379	C-N	Loss of 2 benzyls 289	C-N	Loss of linkage 173	C-N
IL3	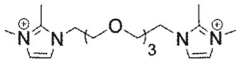	352.25	362	141	C-O	139	C-O	125	C-O
IL4	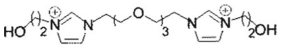	384.24	340	139	C-O	Complete degradation			
IL5	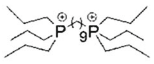	446.42	464[b]	Intact 446 (m/z 223)	None	Dication + NTf_2 726	None	Loss of propyl, gain O 419	C-P oxidation
IL6	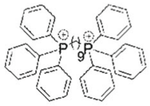	650.83	424[b]	Intact 650 (m/z 325)	None	Dication + NTf_2 930	None	NA	
IL7	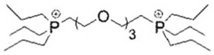	480.39	398	187	C-O	Complete degradation			
IL8	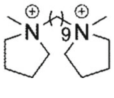	296.32	373[b]	Intact 296 (m/z 148)	None	Loss of methyl 282 (m/z 141)	C-N	Dication + NTf_2 576	None

[a] Temperature of 5% weight loss determined with thermogravimetric analysis (TGA). Conditions: 10 °C/min from room temperature (22 °C) to 600 °C.

[b] T_d temperatures taken from reference [14]

Table 2 MS peaks of the volatiles emitted by dicationic NTf_2 ionic liquids after heating at 400 °C for 30 min under argon flow

IL Code	Peak 1		Peak 2		Peak 3		Peak 4	
	Mass	Broken bond	Mass	Broken bond	Mass	Broken bond	Mass	Broken bond
IL1	207	C-N imidazole C-C methylene	221	C-N imidazole	193	C-N imidazole + 2 C-C methylene	167	C-N imidazole + 4 C-C methylene
IL2	173	C-N benzyl imidazole	207	As 1 + C-N benzyl	209	As 2 + C-C methylene	297	C-N loss of benzyl imidazole
IL3	125	C-N and C-O bonds	139	C-N and C-O bonds	141	C-N, C-C, and C-O bonds	153	C-N, C-O
IL4	244	C-N and C-O bonds	322 (*m*/*z* 161)	C-C bonds	139	C-N and C-O bonds	125	C-N and C-O bonds
IL5	199	C-P + oxidation	285	C-P	223	None	375	C-P + oxidation
IL6	683 (*m*/*z* 341)	dioxidized IL	387	C-P	373	C-P + C-C methylene	301	C-P + oxidation
IL7	453	C-P + oxidation	187	C-P and C-O bonds	161	C-P, tripropyl phosphonium	199	C-P
IL8	198	C-N pyrrolidine + C-C methylene	196	C-N pyrrolidine + C-C methylene	184	C-N pyrrolidine + 2 C-C methylene	170	C-N pyrrolidine + 3 C-C methylene

see ESM for mass spectra

in case of ammonium and imidazolium cations paired with halide ions [39, 46, 51, 52]. Since halides being more nucleophilic, the reaction can occur at lower temperatures (< 100 °C), decreasing the thermal stability of ILs. [39] The NTf_2 anion is less nucleophilic compared to the halides, which provides higher thermal stabilities and the reverse Menshutkin reaction occurs at higher temperatures (> 350 °C). Further fragmentation was observed with loss of methylene groups from the alkyl chain with intervals of *m*/*z* 14 (Fig. 1c and see ESM Fig. S6). The sequential loss of CH_2 groups is a characteristic feature of alkanes observed under electron ionization experiments [53].

Figure 2 shows the mass spectra of the original IL5 (Fig. 2a), the IL5 residue (Fig. 2b) collected after heating at 400 °C, and the collected IL5 volatiles after 30 min of heating at 400 °C (Fig. 2c). An important point to note is that the mass spectra of the collected volatiles of phosphonium ILs with alkyl (C_9) linkage, IL5, and IL6 showed small peaks at respectively *m*/*z* 223 and 325 (Fig. 2c and ESM Figs. S18 and S21). They correspond to the intact dicationic IL demonstrating the possibility of volatile NIP formation for these two ILs. The mass spectrum of the collected volatiles was more complex compared to the residual IL and showed multiple fragments due to the breaking of C-P bonds and C-C bonds (Table 2, Fig. 2). The mass spectra of residual IL5 and collected volatiles showed peaks at *m*/*z* 419 and 199. The peaks were of interest, as they belonged to the formation of oxides by IL5 at high temperatures. The possible mechanism for the formation of phosphine oxides is shown in Fig. 3. Despite the inert atmosphere, trace moisture content of the argon may have led to the oxide formation. The formation of phosphine oxides was also observed during the thermal degradation study of quaternary phosphonium-based montmorillonites [54, 55]. Like IL5, IL6 also showed the formation of oxides at high temperatures (see ESM Figs. S19 and S21). The results for IL6 were similar to IL1, with a practically unchanged mass spectrum compared to the original IL, and a spectrum of the trace collected volatiles showing phosphorus oxidation and some thermal breakings (Table 2) (see ESM Figs. S19 and S21).

The six other ILs had different behaviors. For IL2, IL5, and IL8, the original IL peak, observed before heating, was still visible in the spectrum of the heated residual IL (see ESM Figs. S8, S17, and S26). However, it was not the highest peak and was accompanied by several peaks denoting partial but significant thermal decomposition. Indeed, the corresponding spectra of the collected fumes showed a wealth of IL thermal fragments (Table 2) (see ESM Figs. S7, S16, and S25).

IL3, IL4, and IL7, the ILs with a three-unit PEG spacer, were completely destroyed by 30 min heating at 400 °C. Table 1 lists the *m*/*z* values of major peaks seen in the crowded MS spectra obtained by infusing the methanol solution that washed the black carbonaceous material remaining in the vial. The PEG-linked ILs started decomposing at about 300 °C as fragments due to the breaking of C-O bonds (possible mechanism shown in the Fig. 4) were observed in the mass spectra of collected volatiles at 300 °C. The decomposition at lower temperatures can also be seen with lower T_d temperatures of all three PEG ILs (Table 2).

To complete this study, the 400 °C-resistant ILs, i.e., IL1, IL2, IL5, IL6, and IL8, were submitted to a 440 °C test. For each IL, an ampoule containing 0.2 mL of IL was sealed under argon and placed in an oven able to generate a 440 °C regulated temperature. A second ampoule was similarly prepared in the air (no argon purging) and 440 °C heating. IL2 and IL8 were completely decomposed by heating at 440 °C for 30 min leaving black solid material in the vials. The IL5 and IL6 MS

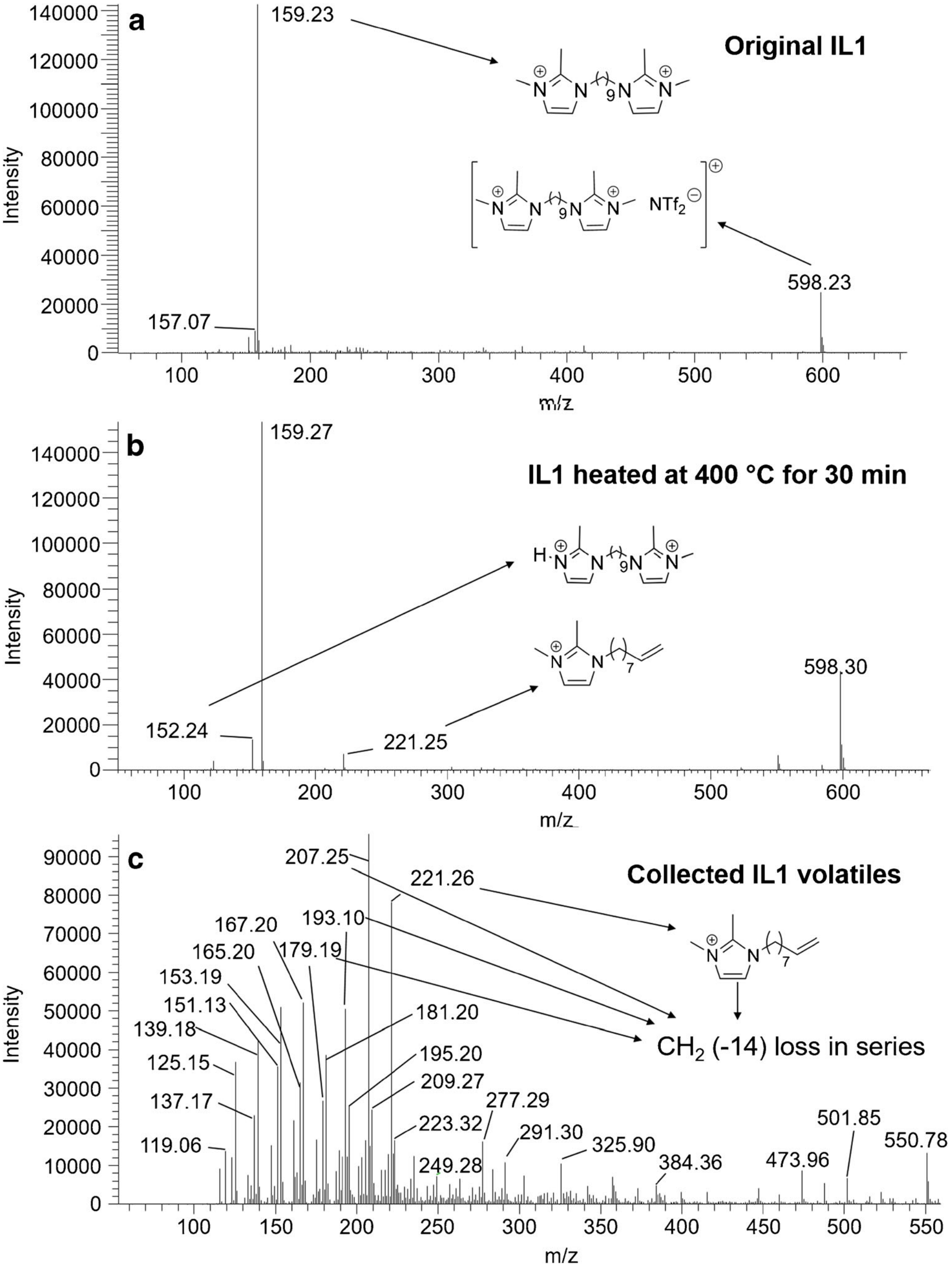

Fig. 1 Mass spectra of IL1. **a** Original IL. **b** Residual IL1 after heating at 400 °C for 30 min. **c** Methanolic solution of collected IL1 volatiles after heating at 400 °C for 30 min. See ESM Fig. S6 for all possible IL1 fragments

base peaks, corresponding to the intact phosphonium dicationic ILs with C_9 spacer were observed (see ESM Fig. S16). The intensity of the *m/z* 419 (IL5) peak (oxidized IL) was, not surprisingly, much higher under air than under argon heating (see ESM Figs. S16 and S17). IL1 showed some darkening color but seemed to mostly withstand the 440 °C temperature both under argon and air (see ESM Figs. S4 and S5). There was more degradation under air than under argon as seen by the darker color of heated IL1 and the lower solubility of the residual material in methanol. However, the two mass spectra of the extracted methanolic solutions still showed the intact IL1 peak and some degradation fragments (see ESM Figs. S4 and S5).

The decomposition studies on dicationic ILs led to some specific observations: the ether bond present in the PEG linkage is the most thermally fragile. The next bond that seems to break under thermal stress is the C-N bond followed by C-C bonds. This order does not follow the strength of chemical bonds that is 358, 348, and 293 kJ/mol for the C-O, C-C, and C-N bond, respectively [56]. The listed strength of the C-P bond, 264 kJ/mol, is even weaker than the C-N bond. However, it seems that the phosphorus-based dicationic ILs are thermally stable, being able to form NIPs with two NTf_2 anions. The probability of cleavage of a particular bond not only depends on the bond strengths but also on the stability of

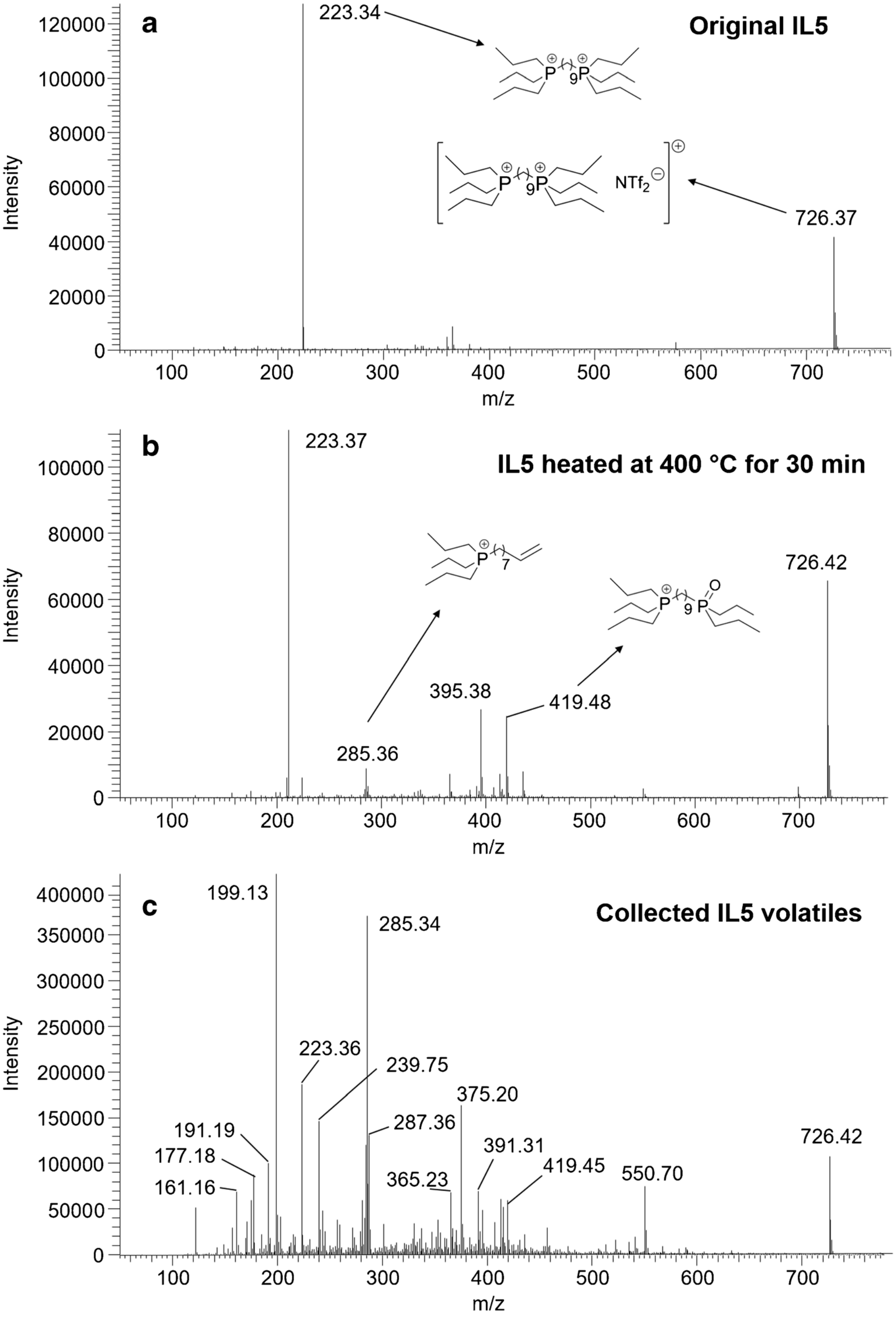

Fig. 2 Mass spectra of IL5. **a** Original IL. **b** Residual IL5 after heating at 400 °C for 30 min. **c** Methanolic solution of collected IL5 volatiles after heating at 400 °C for 30 min. See ESM Fig. S18 for all possible IL5 fragments

the fragments formed in the fragmentation process [53]. The rupture of the C-P bond may be initiated by oxidation by trace amounts of oxygen present in our set-up, inducing the thermal breakdown of phosphonium-based dicationic IL5 and IL6. It is worth mentioning that the thermal decomposition temperature is the upper limit of the liquid range of ILs and is much higher than the boiling points and decomposition temperatures of starting materials (*N*-methyl pyrrolidine: bp = 81 °C, tripropyl phosphine: bp = 187.5 °C, dibromoalkanes: bp range = 167 to 286 °C, tetraethylene glycol: bp = 330 °C with extreme decomposition) [37, 38, 57]. The lower volatilities of ionic liquids (salts) are due to the increased electrostatic and intermolecular interactions as is well-known [37, 39, 58].

Fig. 3 Postulated mechanism for the decomposition of ILs. **a** Imidazolium-based ILs. **b** Phosphonium-based ILs

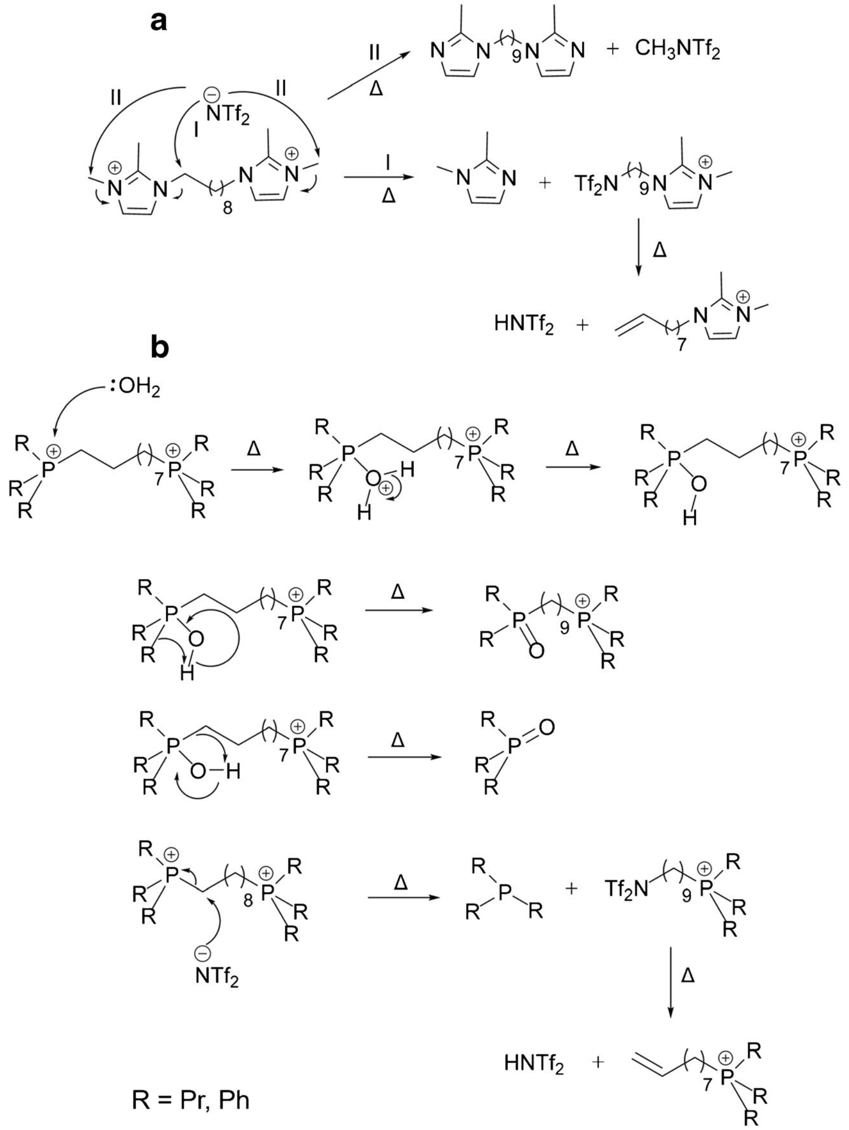

Fig. 4 Postulated mechanism for the thermal decomposition of PEG-linked ILs

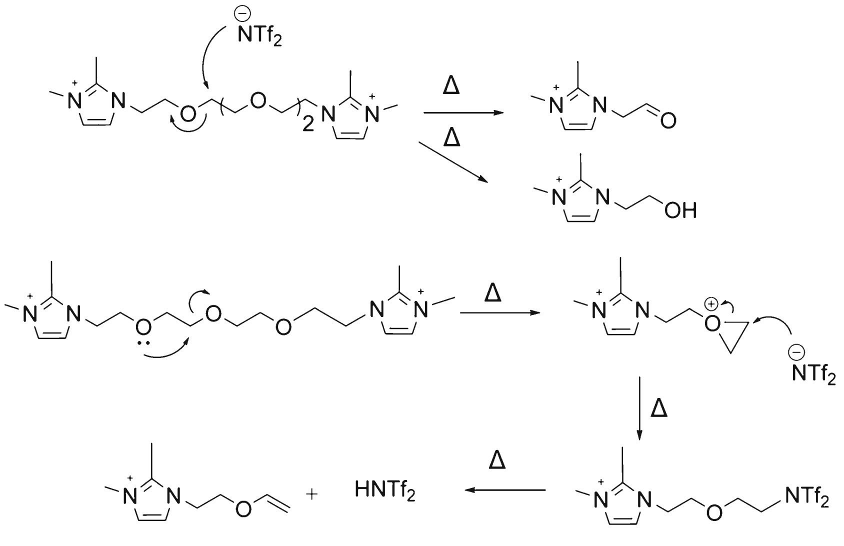

Table 3 MS peaks of volatile dicationic NTf_2-branched ionic liquids seen after heating at 400 °C for 30 min under argon flow

IL code	Dication structure	Dication m.w.	T_d[a] °C	Peak 1		Peak 2		Peak 3	
				Mass	Broken bond	Mass	Broken bond	Mass	Broken bond
IL9	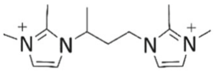	248.37	406	151	C-N imidazole	137	C-N imidazole + C-C methylene	NA	
IL10	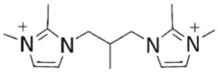	248.37	438	151	C-N imidazole	137	C-N imidazole + C-C methylene	NA	
IL11	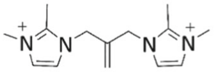	246.36	437	137	C-C methylene	151	C-N imidazole	NA	
IL12	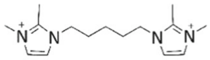	262.40	438	165	C-N imidazole	151	C-N imidazole + C-C methylene	NA	
IL13	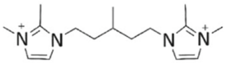	276.43	440	179	C-N imidazole	165	C-N imidazole + C-C methylene	151	C-N imidazole + 2 C-C methylene
IL14	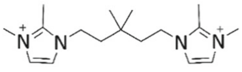	290.45	423	193	C-N imidazole	179	C-N imidazole + C-C methylene	NA	
IL15	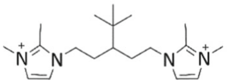	318.51	429	207	C-C methylene	221	C-N imidazole	165	C-N imidazole + C-C *tert*-butyl

[a] Temperature of 5% weight loss determined with thermogravimetric analysis (TGA). Conditions: 10 °C/min from room temperature (22 °C) to 600 °C

Analysis of branched chain linkage ILs

To understand the effect of substituted linkage chains on the thermal stabilities of dicationic ILs, the degradation study was extended to a selection of C_3- and C_5-branched chain dicationic ILs. Table 3 summarizes the data obtained by the degradation study of six branched chain ILs and one linear analog, IL9 to IL15.

C_3-branched ILs

The α-(IL9) and β-(IL10) substituted C_3-linked branched ILs showed similar mass spectra for the collected volatiles at 400 °C (see ESM Figs. S28 and S30). The peak at *m*/*z* 151 was the highest in intensity and belonged to the fragment formed from of breaking of C-N bonds. The *m*/*z* 151 peak was also present in the mass spectrum obtained from the analysis of volatile fragments of IL9 collected at 300 °C. However, the same fragment was absent in the mass spectrum of collected volatiles of IL10 at 300 °C. This shows that the presence of methyl group on the α-carbon provided extra stability to the carbocation of the broken fragment. This is also supported by the decreased T_d temperature of IL9 (406 °C) compared to IL10 (438 °C). In the case of IL11 with an external double bond on the C2 carbon, the fragment with *m*/*z* 137 was the base peak, and the fragment due to breaking of C-N bond (*m*/*z* 151) was about one third the intensity of the base peak (see ESM Fig. S32). The double bond on the C2 carbon may have accelerated the breaking of the C1-C2 bond.

C_5-branched ILs

Four ILs with different substitutions patterns on the C_5-branched linkages were analyzed. IL13, IL14, and IL15 contain a methyl, dimethyl, and a tert-butyl substituent on the central carbon (C3) of the C_5 linkage, respectively. The fragmentation pattern of IL12 was similar to IL1 (both straight chain-linked ILs), with the breaking of the C-N bond (base peak at *m*/*z* 165) and further loss of $-CH_2$ groups in series (see ESM Figs. S34 and S35). IL13 and

IL15 (both with single substituents on the C3 carbon) showed similar fragmentation pattern with major peaks belonging to the breaking of the C-N bond, C1-C2 bond, and C2-C3 bond (see ESM Figs. S36, S37, S40, and S41). The presence of methyl and tert-butyl substituent on the C3 carbon may have accelerated the breaking of the C2-C3 bond as fragments at *m*/*z* 165 and 207 were base peaks (see ESM Figs. S36 and S40). These fragments must be the daughter fragments of a parent fragment obtained by the breaking of a C-N bond (fragments at *m*/*z* 179 and 221) of the intact IL. The T_d temperatures of IL12 and IL13 are close (438 and 440 °C, respectively) which means that the C2-C3 bond must have broken after the cleavage of the C-N bond. The breaking of *tert*-butyl substituent was also observed in the case of IL15 as it is a good leaving group, and this might be the reason for the lower T_d temp of IL15 (429 °C) compared to IL12. Interestingly, IL14 showed a different degradation pattern compared to the IL13 and IL15. The mass spectrum of the volatiles of IL14 (T_d = 423 °C) was cleaner than the mass spectra of IL13 and IL15 (see ESM Fig. S38). The base peak observed at the *m*/*z* 193 was due to the breaking of C-N bond and a less intense peak observed at *m*/*z* 179 was may be due to the breaking of one of the methyl substituents on the C3 carbon. Removal of one methyl group leads to the formation of stable tertiary carbocation which might be the reason for its cleavage and the lower T_d temperature of IL14 compared to IL13.

Conclusions

The results of the degradation study led to the following observations: (1) only the phosphonium-based ILs formed volatile NIPs found in the collected "volatile fractions." All other tested dicationic ILs have undetectable volatility at 400 °C with no NIP formation. (2) All the studied ILs show at least some decomposition at 400 °C, but with considerable differences in magnitude. The dicationic ILs decompose even when their observed TGA temperature (T_d) is much higher than 400 °C (e.g., 467 and 464 °C for IL1 and IL5, respectively; Table 1). (3) All three studied dicationic ILs with a PEG spacer were completely destroyed in less than 30 min at 400 °C with the prolific breaking of C-O bonds. (4) The phosphonium-based dicationic ILs are sensitive to P-oxidation at higher temperatures. (5) The bis-dimethylimidazolium IL1 with a nonyl (C_9) spacer was remarkably thermally resistant even in the presence of oxygen. (6) The position and number of substituents on the linkage chain affects the degradation pattern and stabilities of ILs, as the presence of one substituent on the central carbon of the C-5 linkage accelerated the breaking of the C2-C3 bond. Whereas, the presence of two substituents on the C3 carbon leads to removal of one of the substituents and a further decrease in thermal stability. (7) The breaking of bonds under thermal stress studies did not follow the order of bond strengths and may be dependent on other factors such as the stability of fragments and the influence of substituents. (8) The heteroatom-carbon single bonds were more prone to thermal decomposition, and the order of thermal breaking was observed to be C-O < C-N < C-P in the studied ILs. In high-temperature applications, to be sure that dicationic ILs are stable and remain in a condensed state, it is recommended that their maximum working temperature be at least 100 °C or in some cases even lower than their experimental TGA decomposition temperatures.

Acknowledgements We acknowledge the Robert A. Welch Foundation (Y0026) for funding this work.

Compliance with ethical standards

Conflicts of interest The authors declare that they have no conflict of interest.

Ethical approval This article does not contain any studies with human or animal subjects.

References

1. Welton T. Room-temperature ionic liquids. Solvents for synthesis and catalysis. Chem Rev. 1999;99(8):2071–84.
2. Han X, Armstrong DW. Ionic liquids in separations. Acc Chem Res. 2007;40(11):1079–86.
3. Ho TD, Zhang C, Hantao LW, Anderson JL. Ionic liquids in analytical chemistry: fundamentals, advances, and perspectives. Anal Chem. 2013;86(1):262–85.
4. Soukup-Hein RJ, Warnke MM, Armstrong DW. Ionic liquids in analytical chemistry. Annu Rev Anal Chem. 2009;2:145–68.
5. Meng Y, Pino V, Anderson JL. Exploiting the versatility of ionic liquids in separation science: determination of low-volatility aliphatic hydrocarbons and fatty acid methyl esters using headspace solid-phase microextraction coupled to gas chromatography. Anal Chem. 2009;81(16):7107–12.
6. Li T, Joshi MD, Ronning DR, Anderson JL. Ionic liquids as solvents for in situ dispersive liquid–liquid microextraction of DNA. J Chromatogr A. 2013;1272:8–14.
7. Armstrong DW, Zhang L-K, He L, Gross ML. Ionic liquids as matrixes for matrix-assisted laser desorption/ionization mass spectrometry. Anal Chem. 2001;73(15):3679–86.
8. Carda-Broch S, Berthod A, Armstrong DW. Ionic matrices for matrix-assisted laser desorption/ionization time-of-flight detection of DNA oligomers. Rapid Commun Mass Spectrom. 2003;17(6):553–60.
9. Tholey A, Heinzle E. Ionic (liquid) matrices for matrix-assisted laser desorption/ionization mass spectrometry—applications and perspectives. Anal Bioanal Chem. 2006;386(1):24–37.
10. Chang YL, Lee YC, Yang WB, Chen CH. Ionic liquid-assisted electrospray ionization of polysaccharides. J Mass Spectrom. 2011;46(4):367–75.

11. Enders Dickinson V, Williams ME, Hendrickson SM, Masui H, Murray RW. Hybrid redox polyether melts based on polyether-tailed counterions. J Am Chem Soc. 1999;121(4):613–6.
12. Nanayakkara YS, Moon H, Payagala T, Wijeratne AB, Crank JA, Sharma PS, et al. A fundamental study on electrowetting by traditional and multifunctional ionic liquids: possible use in electrowetting on dielectric-based microfluidic applications. Anal Chem. 2008;80(20):7690–8.
13. Bhattacharya B, Samanta A. Excited-state proton-transfer dynamics of 7-hydroxyquinoline in room temperature ionic liquids. J Phys Chem B. 2008;112(33):10101–6.
14. Qiu H, Liang X, Sun M, Jiang S. Development of silica-based stationary phases for high-performance liquid chromatography. Anal Bioanal Chem. 2011;399(10):3307–22.
15. Shu Juan L, Feng Z, Xiao Hua X, Liang Z, Xia L. Surface confined ionic liquid—a new stationary phase for the separation of ephedrines in high-performance liquid chromatography. Chin Chem Lett. 2004;15(9):1060–2.
16. Xu Y, Wang E. Ionic liquids used in and analyzed by capillary and microchip electrophoresis. J Chromatogr A. 2009;1216(24):4817–23.
17. Mendes A, Branco LC, Morais C, Simplício AL. Electroosmotic flow modulation in capillary electrophoresis by organic cations from ionic liquids. Electrophoresis. 2012;33(7):1182–90.
18. Wu B, Reddy R, Rogers R. Novel ionic liquid thermal storage for solar thermal electric power systems, *Proceedings of Solar Forum 2001 Solar Energy: The Power to Choose*, Washington, DC. (2001).
19. Jin C-M, Ye C, Phillips BS, Zabinski JS, Liu X, Liu W, et al. Polyethylene glycol functionalized dicationic ionic liquids with alkyl or polyfluoroalkyl substituents as high temperature lubricants. J Mater Chem. 2006;16(16):1529–35.
20. Minami I, Kamimura H, Mori S. Thermo-oxidative stability of ionic liquids as lubricating fluids. Lubr Sci. 2007;24(3):135–47.
21. Qu J, Blau PJ, Dai S, Luo H, Meyer HM. Ionic liquids as novel lubricants and additives for diesel engine applications. Tribol Lett. 2009;35(3):181–9.
22. Qu J, Bansal DG, Yu B, Howe JY, Luo H, Dai S, et al. Antiwear performance and mechanism of an oil-miscible ionic liquid as a lubricant additive. ACS Appl Mater Interfaces. 2012;4(2):997–1002.
23. Han X, Armstrong DW. Using geminal dicationic ionic liquids as solvents for high-temperature organic reactions. Org Lett. 2005;7(19):4205–8.
24. Bhawal SS, Patil RA, Armstrong DW. Rapid, effective deprotection of tert-butoxycarbonyl (Boc) amino acids and peptides at high temperatures using a thermally stable ionic liquid. RSC Adv. 2015;5(116):95854–6.
25. Xiao J-C, Shreeve JM. Synthesis of 2, 2’-biimidazolium-based ionic liquids: use as a new reaction medium and ligand for palladium-catalyzed suzuki cross-coupling reactions. J Org Chem. 2005;70(8):3072–8.
26. Anderson JL, Armstrong DW. High-stability ionic liquids. A new class of stationary phases for gas chromatography. Anal Chem. 2003;75(18):4851–8.
27. Breitbach ZS, Armstrong DW. Characterization of phosphonium ionic liquids through a linear solvation energy relationship and their use as GLC stationary phases. Anal Bioanal Chem. 2008;390(6):1605–17.
28. Patil RA, Talebi M, Sidisky LM, Armstrong DW. Examination of selectivities of thermally stable geminal dicationic ionic liquids by structural modification. Chromatographia. 2017;80(10):1563–74.
29. Ho TD, Yehl PM, Chetwyn NP, Wang J, Anderson JL, Zhong Q. Determination of trace level genotoxic impurities in small molecule drug substances using conventional headspace gas chromatography with contemporary ionic liquid diluents and electron capture detection. J Chromatogr A. 2014;1361:217–28.
30. Nacham O, Ho TD, Anderson JL, Webster GK. Use of ionic liquids as headspace gas chromatography diluents for the analysis of residual solvents in pharmaceuticals. J Pharm Biomed Anal. 2017;145:879–86.
31. Frink LA, Weatherly CA, Armstrong DW. Water determination in active pharmaceutical ingredients using ionic liquid headspace gas chromatography and two different detection protocols. J Pharm Biomed Anal. 2014;94:111–7.
32. Frink LA, Armstrong DW. Water determination in solid pharmaceutical products utilizing ionic liquids and headspace gas chromatography. J Pharm Sci. 2016;105(8):2288–92.
33. Lin X, Kavian R, Lu Y, Hu Q, Shao-Horn Y, Grinstaff MW. Thermally-responsive, nonflammable phosphonium ionic liquid electrolytes for lithium metal batteries: operating at 100 degrees celsius. Chem Sci. 2015;6(11):6601–6. https://doi.org/10.1039/C5SC01518A.
34. Fan X, Wang L. Highly conductive ionic liquids toward high-performance space-lubricating greases. ACS Appl Mater Interfaces. 2014;6(16):14660–71.
35. Liu X, Pu J, Wang L, Xue Q. Novel DLC/ionic liquid/graphene nanocomposite coatings towards high-vacuum related space applications. J Mater Chem A. 2013;1(11):3797–809.
36. Zhou F, Liang Y, Liu W. Ionic liquid lubricants: designed chemistry for engineering applications. Chem Soc Rev. 2009;38(9):2590–9.
37. Anderson JL, Ding R, Ellern A, Armstrong DW. Structure and properties of high stability geminal dicationic ionic liquids. J Am Chem Soc. 2005;127(2):593–604.
38. Patil RA, Talebi M, Xu C, Bhawal SS, Armstrong DW. Synthesis of thermally stable geminal dicationic ionic liquids and related ionic compounds: an examination of physicochemical properties by structural modification. Chem Mater. 2016;28(12):4315–23.
39. Maton C, De Vos N, Stevens CV. Ionic liquid thermal stabilities: decomposition mechanisms and analysis tools. Chem Soc Rev. 2013;42(13):5963–77.
40. Payagala T, Huang J, Breitbach ZS, Sharma PS, Armstrong DW. Unsymmetrical dicationic ionic liquids: manipulation of physicochemical properties using specific structural architectures. Chem Mater. 2007;19(24):5848–50.
41. Wasserscheid P, Welton T. Ionic liquids in synthesis. Weinheim: Wiley-VCH Verlag GmbH & Co. KGaA; 2008.
42. Clough MT, Geyer K, Hunt PA, Mertes J, Welton T. Thermal decomposition of carboxylate ionic liquids: trends and mechanisms. PCCP. 2013;15(47):20480–95.
43. Lovelock KR, Armstrong JP, Licence P, Jones RG. Vaporisation and thermal decomposition of dialkylimidazolium halide ion ionic liquids. PCCP. 2014;16(4):1339–53.
44. Nevshupa R, Conte M, Guerra S, Roman E. Time-resolved characterization of dynamic tribochemical processes for dicationic imidazolium ionic liquid. Lubricants. 2017;5(3):27.
45. Clough MT, Crick CR, Grasvik J, Hunt PA, Niedermeyer H, Welton T, et al. A physicochemical investigation of ionic liquid mixtures. Chem Sci. 2015;6(2):1101–14.
46. Baranyai KJ, Deacon GB, MacFarlane DR, Pringle JM, Scott JL. Thermal degradation of ionic liquids at elevated temperatures. Aust J Chem. 2004;57(2):145–7.
47. Ohtani H, Ishimura S, Kumai M. Thermal decomposition behaviors of imidazolium-type ionic liquids studied by pyrolysis-gas chromatography. Anal Sci. 2008;24(10):1335–40.
48. Wooster TJ, Johanson KM, Fraser KJ, MacFarlane DR, Scott JL. Thermal degradation of cyano containing ionic liquids. Green Chem. 2006;8(8):691–6.
49. Huang K, Han X, Zhang X, Armstrong DW. PEG-linked geminal dicationic ionic liquids as selective, high-stability gas

chromatographic stationary phases. Anal Bioanal Chem. 2007;389(7–8):2265–75.

50. Talebi M, Patil RA, Sidisky LM, Berthod A, Armstrong DW. Branched-chain dicationic ionic liquids for fatty acid methyl ester assessment by gas chromatography. Anal Bioanal Chem. 2017; https://doi.org/10.1007/s00216-017-0722-y.
51. Sawada M, Takai Y, Chong C, Hanafusa T, Misumi S, Tsuno Y. Pyridinium ion reactivities: substituent effect on the reverse Menschutkin reaction of 1-methylpyridinium cations with iodide anion. Tetrahedron Lett. 1985;26(41):5065–8.
52. Ngo HL, LeCompte K, Hargens L, McEwen AB. Thermal properties of imidazolium ionic liquids. Thermochim Acta. 2000;357:97–102.
53. Silverstein RM, Webster FX. Spectrometric identification of organic compounds. New York: John Wiley and Sons; 1998.
54. Ganguly S, Dana K, Mukhopadhyay TK, Ghatak S. Thermal degradation of alkyl triphenyl phosphonium intercalated montmorillonites. J Therm Anal Calorim. 2011;105(1):199–209.
55. Xie W, Xie R, Pan W-P, Hunter D, Koene B, Tan L-S, et al. Thermal stability of quaternary phosphonium modified montmorillonites. Chem Mater. 2002;14(11):4837–45.
56. Cottrell TL. The strengths of chemical bonds. Butterworths: Academic Press; 1958.
57. Glastrup J. Degradation of polyethylene glycol. A study of the reaction mechanism in a model molecule: tetraethylene glycol. Polym Degrad Stab. 1996;52(3):217–22.
58. Cao Y, Mu T. Comprehensive investigation on the thermal stability of 66 ionic liquids by thermogravimetric analysis. Ind Eng Chem Res. 2014;53(20):8651–64.